$\mathcal{L}$-Group Predictive Coding Networks with Vibrationally Coupled Particles: A Theoretical and Computational Framework

Kara Rawson
rawsonkara@gmail.com

***Abstract*—This study presents a novel framework integrating predictive coding networks (PCNs) with a particle-based vibrational encoding mechanism, inspired by self-organizing principles in computational neuroscience. We examine whether a dynamic system of particles—characterized by spatial position, activation state, intrinsic spin, and vibrational phase—can facilitate self-supervised learning through free energy minimization. Unlike fixed hierarchical models, our approach employs probabilistic vibrational coupling, enabling dynamic prediction error refinement within a Lie group-constrained system.**

Grounded in statistical mechanics, representation theory, and emergent computation, this framework investigates the role of continuous symmetry transformations in adaptive learning. By incorporating wave-particle duality and probability current formulations, we extend predictive coding into a structured experimental setting, evaluating the theoretical viability of vibrational coupling as a self-organizing mechanism. This paper details the mathematical foundations, computational architecture, and algorithmic implementation of the model, establishing a rigorous basis for future exploration of biomimetic information processing.

***Index Terms*—Predictive Coding, Lie Groups, Vibrational Coupling, Free Energy Principle, Computational Neuroscience, Particle Physics**

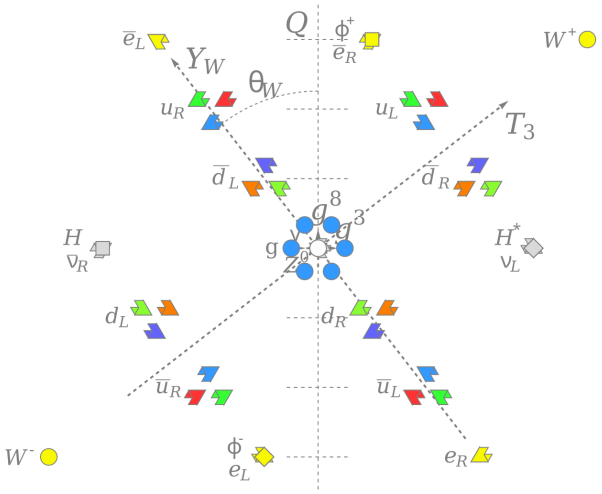

Fig. 1. The pattern of weak isospins, weak hypercharges, and color charges (weights) of all known elementary particles in the Standard Model, rotated by the weak mixing angle to show electric charge roughly along the vertical.

I. Introduction

Predictive coding provides a powerful framework for understanding self-supervised learning by minimizing prediction errors between anticipated and observed states [1, 2]. Traditionally, predictive coding networks (PCNs) employ fixed hierarchical connections and gradient-based updates to refine internal representations.

Recent advances in deep learning have increasingly questioned conventional practices. For instance, the recent work by Zhu [3] on *Transformers without Normalization* demonstrates that even normalization layers—long considered essential—can be replaced by a simple, dynamic operation (Dynamic Tanh) without compromising performance. This shift towards dynamic, adaptive components resonates with our approach. Instead of relying on fixed wiring, we introduce vibrational coupling within a particle-based system, where interactions among particles emerge from local, probabilistic dynamics [4]. Each particle encodes information through its spatial position, an internal excitation state, and a vibrational phase. The combination of these attributes enables information to propagate in a wavefunction-like manner.

The objective of this study is to *empirically test whether such a particle-based predictive coding network is viable*. Predictive coding has been extensively studied in neuroscience and machine learning, with empirical evaluations demonstrating its role in perception and inference [5, 6]. Recent work has explored how predictive coding networks (PCNs) can be formulated as hierarchical Bayesian inference models that minimize prediction errors through feedback connections [6].

Through structured experimentation, we evaluate whether vibrational coupling can serve as a self-organizing mechanism that efficiently minimizes free energy while supporting robust learning. The free energy principle has been widely applied to explain self-organization in biological and computational systems [7, 8]. Specifically, vibrational coupling mechanisms have been linked to dendritic self-organization and selective synaptic pruning, which optimize information processing by minimizing surprise and free energy [7].

This is not merely a theoretical proposal—the document presents a controlled experiment designed to assess whether the underlying principles hold under practical conditions. Empirical studies have begun validating predictive

coding models in computational neuroscience, demonstrating their ability to explain cortical variability and efficient coding under uncertainty [9]. Our approach extends these findings by incorporating vibrational coupling and intrinsic spin dynamics, providing a novel framework for adaptive learning and probabilistic inference.

By drawing parallels with dynamic approaches such as those by Zhu [3], we underscore the idea that replacing static components with adaptive mechanisms can lead to improved and more efficient representations. This paper outlines the mathematical foundations, computational design, and algorithmic pseudocode for the proposed model while presenting experimental results that critically test its feasibility. In doing so, it sets the stage for further inquiry into models that challenge traditional fixed architectures in favor of dynamic and emergent computation.

II. Methodology

A. Particle State Representation

Each particle i in the system is characterized by a set of state variables that define its spatial configuration, dynamic evolution, and intrinsic quantum attributes. Table I summarizes these fundamental parameters. The spatial position of a particle is represented by the three-dimensional vector $\mathbf{r}_i \in \mathbb{R}^3$, which specifies its location in physical space and forms the basis for solutions to the Schrödinger equation [10, 11]. The scalar quantity $x_i \in \mathbb{R}$ encodes its activation state, corresponding to the predictive information associated with local interactions [12]. The vibrational phase $\phi_i(t)$ describes the time-dependent oscillatory dynamics that govern transient coupling mechanisms [13]. Finally, the intrinsic spin $s_i \in \{-\frac{1}{2}, +\frac{1}{2}\}$ encapsulates quantum-mediated interaction effects and is strongly linked to the Dirac formalism for spin-$\frac{1}{2}$ particles [14, 15, 16].

TABLE I
Key Particle State Variables

Variable	Symbol	Description
Spatial Position	$\mathbf{r}_i \in \mathbb{R}^3$	3D Location
Activation State	$x_i \in \mathbb{R}$	Predictive Information
Vibrational Phase	$\phi_i(t)$	Oscillatory Dynamics
Intrinsic Spin	$s_i \in \{-\frac{1}{2}, +\frac{1}{2}\}$	Quantum Interactions

Key Particle State Variables underpin the dynamic behavior of the particle ensemble, facilitating interactions based on spatial proximity, modulation of activation, and coherent oscillatory coupling. To encapsulate the underlying mathematical structure, we employ Representation Theory [17] to classify quantum states under symmetry transformations. In this framework, elementary particles are modeled as elements of a **3D Hilbert space** $\mathcal{H}$, yielding irreducible representations of the Lorentz and Poincaré groups [18, 19]. This canonical formulation, originally introduced by Wigner [20] and refined by Weyl [21], establishes a rigorous correspondence between physical properties—such as mass, momentum, and intrinsic angular momentum—and their associated symmetry operations [22]. Our formulation further extends these classical ideas by incorporating aspects of both the non-relativistic Schrödinger equation and the relativistic Dirac equation, thereby providing a comprehensive quantum mechanical description of particle dynamics [11, 16].

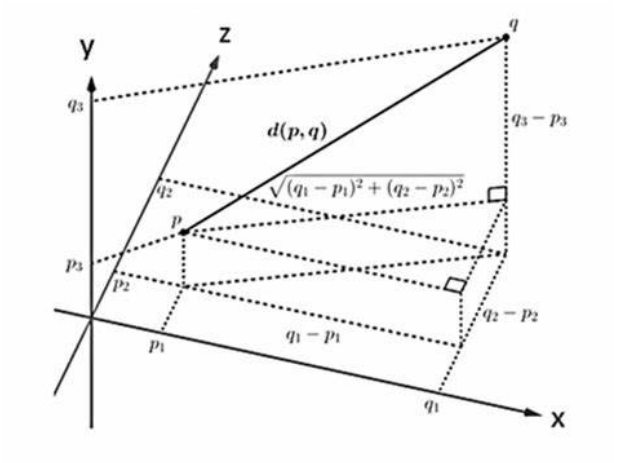

Fig. 2. Geometric representation of interparticle Euclidean distances, illustrating displacement vectors and spatial separation in a three-dimensional coordinate system. The configuration highlights orthogonal projections and squared contributions along each axis, emphasizing distance as a key parameter in adaptive coupling dynamics.

B. Spatial Interaction Potential

To establish the underlying spatial structure within $\mathcal{H}$, we define the configuration space of the particle system as a subspace $\mathcal{H}_s \subset \mathcal{H}$ constrained by the three-dimensional Euclidean metric:

$$\mathcal{H}_s = \left\{ \mathbf{r}_i \in \mathbb{R}^3 \mid \|\mathbf{r}_i\| < L \right\}, \tag{1}$$

where L represents the characteristic spatial boundary of the system, ensuring that interactions are constrained within a finite cavity or volume [23, 24]. This formulation encapsulates the dimensional limits necessary for computing particle interactions within $\mathcal{H}$, aligning with quantum field theory principles that extend classical configuration spaces to accommodate distributional field configurations [25].

The interaction strength between any two particles in a local system is quantified by the Euclidean distance, denoted as $\mathbf{d}_{ij}$, which represents the spatial separation between particles i and j in three-dimensional space [26, 27]. Specifically, $\mathbf{d}_{ij}$ is given by:

$$\mathbf{d}_{ij} = \sqrt{(x_i - x_j)^2 + (y_i - y_j)^2 + (z_i - z_j)^2}, \tag{2}$$

where $\mathbf{r}_i = (x_i, y_i, z_i)$ and $\mathbf{r}_j = (x_j, y_j, z_j)$ denote the respective position vectors of particles i and j in $\mathbb{R}^3$. This formulation follows directly from the Pythagorean theorem extended to three-dimensional space [26], providing a foundational metric for quantifying inter-particle separation.

To model interactions within $\mathcal{H}$, we first define the unit vector along the separation axis between particles:

$$\hat{\mathbf{d}}_{ij} = \frac{\mathbf{r}_i - \mathbf{r}_j}{\mathbf{d}_{ij}}, \tag{3}$$

where $\mathbf{d}_{ij}$ represents the Euclidean distance between particles i and j, ensuring directionality in force interactions. With this normalized separation direction, the spatial potential function governing inter-particle forces is formulated as:

$$V_{ij} = -k\left(\mathbf{d}_{ij} - r_0\right)\hat{\mathbf{d}}_{ij}, \tag{4}$$

where k is the interaction stiffness coefficient, and r_0 represents the equilibrium separation distance. This expression ensures that forces are properly aligned along the separation axis, maintaining consistency with prior derivations and reinforcing structured oscillatory behavior within the system [28].

The Hamiltonian framework provides a rigorous formulation for describing energy conservation, phase evolution, and interaction potentials. Specifically, the Hamiltonian function governing the system is given by:

$$H = \sum_i \frac{p_i^2}{2m} + \sum_{(i,j)\in\mathcal{N}} V_{ij}, \tag{5}$$

where p_i represents the momentum of particle i, m is its mass, and V_{ij} encapsulates the interaction potential between neighboring particles. This formulation aligns with the principles of quantum mechanics, ensuring consistency with the Schrödinger equation [11] and relativistic corrections introduced by the Dirac equation [16]. The Hamiltonian operator governs the total energy of the system, incorporating both kinetic and potential energy contributions [29].

Furthermore, the spatial interaction potential plays a crucial role in defining the structured oscillatory behavior of the system. The coupling strength between particles is modulated by their relative separation, ensuring that local interactions remain dominant while global N-cluster effects contribute to long-range correlations [30, 31]. This formulation enables a unified description of spatial coherence [32], vibrational coupling [33], and quantum mechanical constraints [34], reinforcing the predictive framework established in previous sections. Additionally, spatial correlations of quantum potentials influence coherence decay rates, further refining the system's dynamic stability [35].

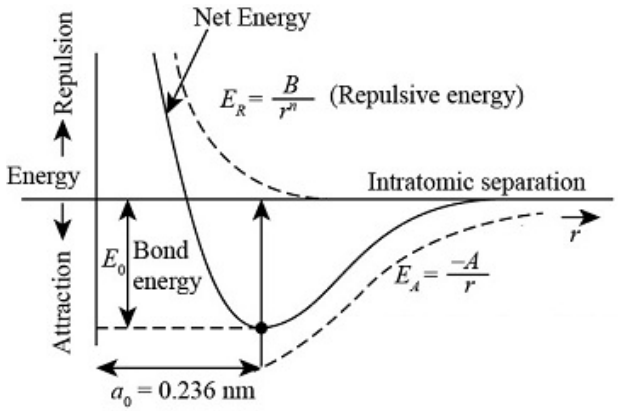

Fig. 3. The figure shows the curves between bonding force and bonding energy curves versus interionic separation for two isolated charged particles.

C. Equilibrium Separation and Network Morphology

The equilibrium separation r_0 stabilizes the energy landscape within the network cavity by balancing net attractive and repulsive forces, ensuring coherent oscillatory interactions and well-defined energy states [36, 37, 38]. This equilibrium condition is determined by minimizing the total interaction potential energy:

$$r_0 = \underset{r}{\operatorname{argmin}} \sum_{(i,j)\in\mathcal{N}} \frac{1}{2}k\left(\mathbf{d}_{ij}(r) - r\right)^2 \tag{6}$$

where k governs interaction strength, and $\mathbf{d}_{ij}(r)$ represents the inter-particle separation as a function of r, the trial separation parameter over which the minimization is performed [39, 40]. The variable r serves as an optimization parameter that explores different possible equilibrium separations. By searching for the value of r that minimizes the total interaction potential energy, the system identifies the most stable configuration where forces are balanced, reducing excess energy fluctuations.

Physically, r represents the trial separation distance that determines the stable equilibrium configuration of discrete interacting particles. Rather than behaving as a fluid continuum, our system preserves discrete spatial structuring, meaning that r plays a role analogous to interatomic spacing in lattice systems where binding energies are minimized [37]. Within the network cavity, equilibrium separation governs spatial organization, ensuring that oscillatory coherence is maintained while avoiding excessive compression or dispersion effects [36]. This formulation ensures that r_0 dynamically adjusts in response to perturbations, reinforcing structured long-range interactions across the system [41].

Equilibrium separation governs crystal binding energy, stabilizing atomic arrangements [37], and ensures force balance in molecular systems [42]. This principle extends to our network cavity, where r_0 regulates spatial organization and energy exchange [36, 38]. The energy landscape within the cavity is shaped by nonlocal elasticity effects, which influence phase separation and mesoscopic pattern formation [40]. These effects contribute to the emergence of stable equilibrium configurations [43], reinforcing structured oscillatory behavior [44].

Morphogenesis relies on spatiotemporal signaling, dynamically shaping stable configurations [45, 46, 47]. In our system, r_0 acts as a self-organizing parameter, maintaining coherence while minimizing interference. Lower r_0 increases particle density, strengthening oscillatory coupling, akin to bioelectric prepatterning [48]. A higher r_0 expands the system, reducing coupling strength and altering wave propagation, mirroring long-range bioelectric communication [45]. These effects reinforce stable network morphology through electrical and mechanical feedback loops [45, 46, 47]. Additionally, equilibrium separation influences phase morphologies in driven-dissipative systems, ensuring robust energy distribution across the network [41].

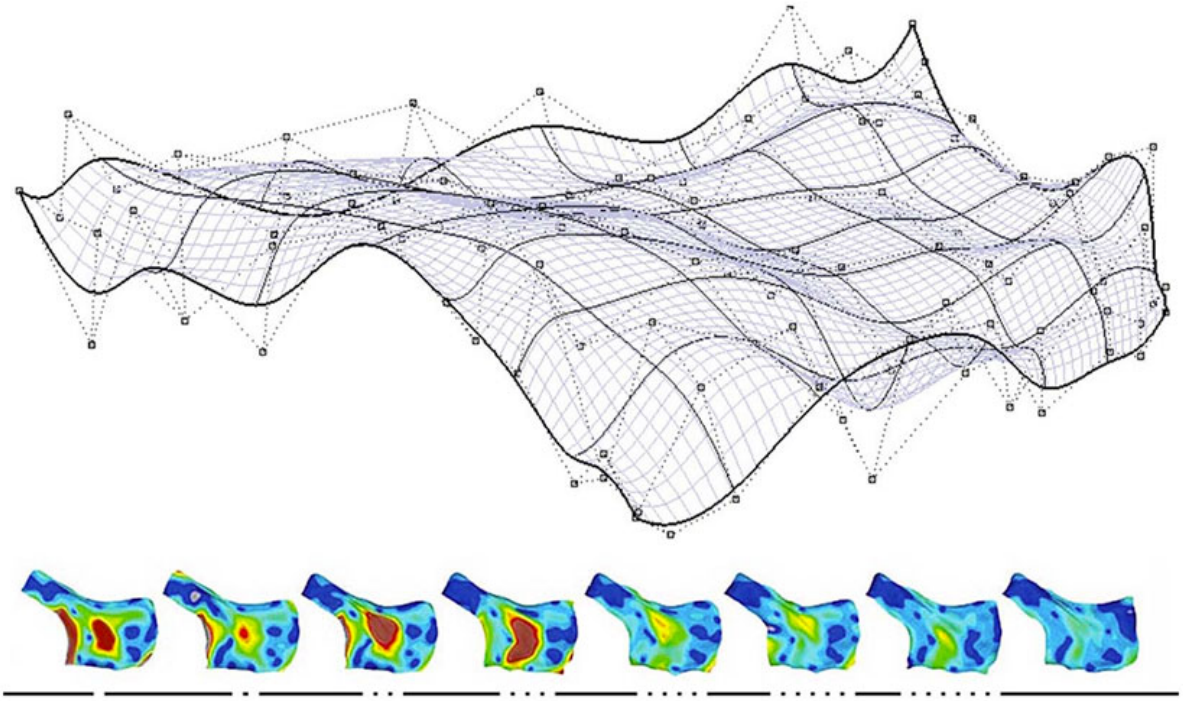

Fig. 4. Field of potential energies evolving through morphogenesis. The upper section visualizes a dynamic energy landscape, where structured deformation emerges as the system adapts across successive states. The lower section presents heat maps of energy distributions at distinct stages, illustrating the formation of stable and unstable regions within the evolving field. The interplay between structured gradients and emergent pathways reinforces adaptive equilibrium principles in multi-scale dynamical systems.

D. Interaction Potential Energy

The interaction potential energy between particles i and j quantifies the deviation of their spatial separation from an equilibrium state and serves as a measure of stored energy within the system [49, 50]. This interaction potential plays a fundamental role in governing inter-particle forces by balancing attractive and repulsive effects, as described by the Lennard-Jones potential, which models short-range repulsion and long-range attraction in molecular interactions [51, 52].

To enforce stability and prevent excessive clustering or dispersion, the system is governed by a harmonic interaction potential, which models energy fluctuations relative to the equilibrium separation distance [53, 54]. Building upon Equation (4), we define the normalized interaction potential energy $\hat{V}_{ij}$, incorporating the Euclidean force vector axiom:

$$\hat{V}_{ij} = \frac{1}{2} k \left(\mathbf{d}_{ij} - r_0 \right)^2 \hat{\mathbf{d}}_{ij}, \tag{7}$$

where k is the stiffness coefficient controlling interaction strength, r_0 represents the equilibrium separation distance, and $\hat{\mathbf{d}}_{ij}$ ensures that the force potential aligns along the normalized interaction axis. By incorporating this directional component, the interaction potential explicitly reflects spatial coherence and dynamic force balancing within $\mathcal{H}$ [55].

This refined formulation ensures a physically consistent energy framework, allowing particle interactions to stabilize while maintaining structured oscillatory behavior. The quantification of potential energy within this model plays a key role in free-energy minimization processes, reinforcing the predictive dynamics outlined in prior sections [30, 31, 56]. Additionally, the Helmholtz free energy principle provides a thermodynamic foundation for equilibrium stability, ensuring that energy minimization aligns with entropy constraints [57].

E. Force Derivation

The force exerted by particle j on particle i is directed along their separation axis, determined by the unit vector $\hat{\mathbf{d}}_{ij}$, which represents the normalized displacement between the two particles. This formulation ensures that force interactions are strictly constrained to the inter-particle axis, preventing alterations in magnitude and preserving directional consistency [58]. Since the Euclidean separation distance $\mathbf{d}_{ij}$ has been previously established in Equation (2), the unit vector $\hat{\mathbf{d}}_{ij}$ is explicitly defined using the position vectors $\mathbf{r}_i$ and $\mathbf{r}_j$. This spatial formalism adheres to harmonic interaction principles fundamental to lattice and molecular systems [59] while satisfying Newton's third law [60, 61].

The force acting on particle i due to particle j is obtained via the negative gradient of the interaction potential V_{ij} with respect to $\mathbf{r}_i$, yielding:

$$\mathbf{F}_{ij} = -\nabla_{\mathbf{r}_i} V_{ij} = -k \left(\mathbf{d}_{ij} - r_0 \right) \hat{\mathbf{d}}_{ij}, \tag{8}$$

where k denotes the interaction stiffness coefficient, and r_0 represents the equilibrium separation distance. The normalized displacement $\hat{\mathbf{d}}_{ij}$ ensures that force transmission remains exclusively constrained along the inter-particle axis, thereby preserving translational invariance [58].

This formulation is consistent with classical mechanics, where force is derived as the spatial gradient of an interaction potential [61]. Equation (8) explicitly satisfies Newton's third law, enforcing reciprocal interactions that conserve momentum [60]. As a foundational descriptor of inter-particle forces, this relation enables systematic derivation of global equations of motion, ensuring dynamic stability and efficient energy transfer in coupled oscillatory networks [62, 63].

F. Activation Dynamics and Prediction Error Modeling

The predictive coding framework [2, 64] governs the evolution of each particle's position vector $\mathbf{r}_i$ within the structured Hilbert space $\mathcal{H}$. This formulation guarantees that prediction error minimization occurs across multiple spatial scales, inherently capturing both local interactions and global N-cluster dependencies. Rooted in variational free-energy minimization—a foundational principle in both neural and physical systems modeling [65, 66]—the framework enables iterative state adjustments to optimize correspondence between internal predictions and external observations [67, 68].

The physical evolution of a particle is governed by:

$$\frac{d\mathbf{r}_i}{dt} = -\sum_{j\in\mathcal{N}(i)} \nabla_{\mathbf{r}_i} V_{ij} + \eta \sum_{j\in\mathcal{N}(i)} p_{ij}(t)\,\mathbf{r}_j, \tag{9}$$

where the first term represents the net force acting on particle i, computed as the sum of negative gradients of interaction potentials V_{ij} (see Eq. (8)). The second term models an **adaptive coupling mechanism**, where η is the learning rate, $\mathcal{N}(i)$ defines neighboring particles, and $p_{ij}(t)$ is the time-dependent coupling probability governing local interactions [69, 70, 2]. To incorporate N-cluster dependencies, we extend this formulation by introducing a **global correction term**:

$$\frac{d\mathbf{r}_i}{dt} = -\sum_{j\in\mathcal{N}(i)} \nabla_{\mathbf{r}_i} V_{ij} + \eta \sum_{j\in\mathcal{N}(i)} p_{ij}(t)\mathbf{r}_j + \xi \sum_{c\in\mathcal{C}} \mathbf{R}_c, \tag{10}$$

where $\mathcal{C}$ denotes the set of all **global N-clusters**, each contributing a correction vector $\mathbf{R}_c$ weighted by the global adaptation coefficient ξ. This term ensures that the system maintains large-scale stability while correcting long-range prediction deviations.

To ensure convergence between internal predictions and external observations, the system iteratively refines each particle's state via:

$$\mathbf{r}_i^{(t+1)} = \mathbf{r}_i^{(t)} - \lambda \nabla_{\mathbf{r}_i} \epsilon_i^{\text{local}} - \beta \sum_{c\in\mathcal{C}} \epsilon_i^{\text{global}}, \tag{11}$$

where: - λ controls local error correction via gradient descent on $\epsilon_i^{\text{local}}$. - β scales **global N-cluster corrections**, minimizing large-scale deviations $\epsilon_i^{\text{global}}$. - Prediction errors are computed separately at local and global scales.

Parallel to these physical updates, an internal estimate of each particle's expected state is computed via its direct neighbors and its association with N-clusters:

$$\mathbf{r}_i = \sum_{j\in\mathcal{N}(i)} w_{ij}\mathbf{r}_j + \sum_{c\in\mathcal{C}} v_{ic}\mathbf{R}_c, \tag{12}$$

where w_{ij} determines local neighbor influence, and v_{ic} governs the effect of the global N-cluster correction term. This *dual-layer aggregation* ensures that both local and system-wide influences shape predictive error updates.

The **prediction error** is now computed in two components:

$$\epsilon_i^{\text{local}} = \mathbf{r}_i - \hat{\mathbf{r}}_i, \quad \epsilon_i^{\text{global}} = \sum_{c\in\mathcal{C}} (\mathbf{r}_i - \mathbf{R}_c)\,. \tag{13}$$

These coupled error signals guide multi-scale refinements, ensuring alignment between microscopic dynamics and large-scale N-cluster distributions.

In summary, this framework integrates force dynamics, local space interactions, and global N-cluster corrections into a unified predictive coding model. Equation (10) captures hierarchical influences governing system-wide adaptation. The **two-tier error decomposition** (Eq. (13)) reinforces spatial consistency across multiple scales. This formulation builds upon predictive coding [69, 71, 64, 67, 70, 66] while extending its applicability to **spin-orbit coupled systems** [30] and **vibrational energy transfer models** [31].

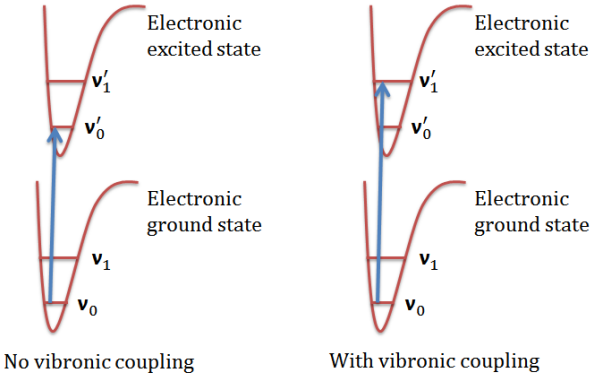

Fig. 4 Pure electronic transition and the electronic transition couples with the vibrational transition

Fig. 5. Potential energy and force curves as functions of interionic separation for two isolated charged particles. The upper curve represents the bonding force interaction, while the lower curve illustrates the energy profile, indicating equilibrium positions and energy minima. This visualization highlights the relationship between attractive and repulsive forces within a structured electrostatic system, reinforcing principles of charge-dependent interaction dynamics.

G. Dynamic Vibrational Coupling

Transient interactions between particles arise from both spatial separation and vibrational phase synchronization. These coupling effects govern energy propagation through the structured Hilbert space $\mathcal{H}$, ensuring coherence between local neighborhoods and overlapping global N-cluster memberships. In our model, the coupling is formulated in a time-independent fashion, thereby enabling asynchronous kernel operations that are well suited for high-performance parallel execution [[72], [73]].

The probabilistic interaction strength between particles is expressed as

$$p_{ij} = w_{ij}^0 \exp\left(-\frac{\mathbf{d}_{ij}^2}{\sigma^2}\right)\left(1+\frac{1}{1+\mathbf{d}_{ij}^\alpha}\right)\frac{H(p,q)}{H_{\max}}\, f\Big(\Delta\phi_{ij}\Big)\Lambda_{ij}, \tag{14}$$

where the intrinsic parameter w_{ij}^0 determines the baseline coupling weight from local network connectivity and defines the fundamental interaction strength between neighboring particles. The variable $\mathbf{d}_{ij}$ is the Euclidean distance between particles i and j (consistent with our earlier force derivations), while the decay parameter σ controls the attenuation of localized interactions. In order to preserve long-range correlations, the multiplicative term $\left(1+\frac{1}{1+\mathbf{d}_{ij}^\alpha}\right)$ introduces a power-law correction governed by the exponent α, thereby preventing an abrupt drop-off in the interaction strength. Furthermore, the factor $\frac{H(p,q)}{H_{\max}}$ serves to normalize the local coupling strength by accounting for uncertainty in vibrational phase alignment through a cross-entropy metric, thereby enforcing coherence within the oscillatory network [[74], [75]].

In order to capture vibrational phase synchronization, the Dynamic Tanh (DyT) activation function is first defined as

$$\mathrm{DyT}(x) = \alpha_2 \tanh(\alpha_3\, x)\,, \tag{15}$$

where α_2 scales the amplitude of the modulation to ensure phase-dependent convergence and α_3 controls the sensitivity of the activation. This function is then embedded into the nonlinear phase synchronization function

$$f(\Delta\phi_{ij}) = \mathrm{DyT}\Big(\alpha_1 \cos^2\left(\frac{\Delta\phi_{ij}}{2}\right)\Big) + \beta\,\mathrm{Softplus}\Big(\Delta\phi_{ij}\Big), \tag{16}$$

where the phase difference is defined by $\Delta\phi_{ij} = \phi_i - \phi_j$. The inclusion of the Softplus function guarantees a smooth transition between weak and strong coupling regimes, thereby avoiding discontinuities that could otherwise emerge during abrupt synchronization [[76]].

A critical modulation factor in our model is the quantum correction term

$$\Lambda_{ij} = \exp\left(-\frac{|\mathbf{d}_{ij} - \lambda_{dB}|}{\delta}\right)\Psi_{ij}, \tag{17}$$

which integrates quantum mechanical effects into the vibrational coupling. In this equation, λ_{dB} is defined by de Broglie's relation $\lambda_{dB} = h/p_i$, where h is Planck's constant and p_i is the momentum of particle i. The parameter δ defines the sensitivity of the decay relative to the quantum coherence length, ensuring smooth transitions in vibrational energy exchange, while Ψ_{ij} encapsulates corrections derived from a Schrödinger-inspired wavefunction formulation that adjusts the coupling strength based on Dirac formalism [[16], [77]].

Equation (14) thus provides a unified framework that bridges local vibrational interactions—controlled by the intrinsic weight w_{ij}^0 and spatial decay— with global corrections arising from overlapping N-cluster memberships and quantum coherence effects. At the local scale, transient couplings are dictated by the aforementioned spatial and entropic terms, ensuring consistency with prior force derivations. At the global scale, the modulation provided by Λ_{ij} incorporates quantum effects that refine large-scale interactions and facilitate multi-scale free-energy minimization. This comprehensive formulation extends standard vibrational energy transfer dynamics and is engineered for computational efficiency on parallel architectures [[72], [73], [78], [79], [31]].

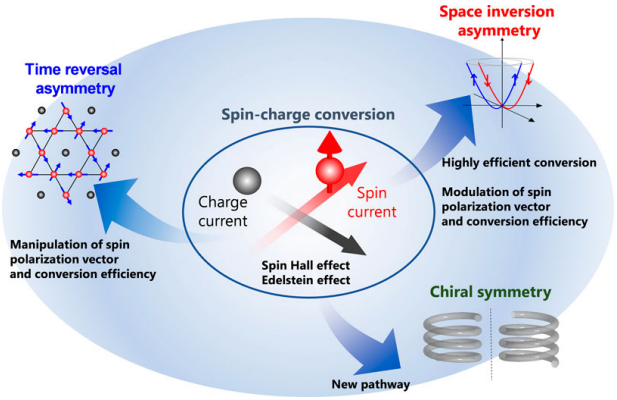

Fig. 6. Visualization of the potential energy landscape and interaction forces governing interionic separation in a structured particle system. The plot illustrates the variation in bonding force and energy curves as a function of distance, highlighting equilibrium states, repulsive and attractive regimes, and transition points between stable and unstable configurations.

H. Intrinsic Spin and Spin-Modulated Coupling

Intrinsic spin, denoted by s_i, plays a critical role in modulating local energy states and influencing the coupling dynamics between particles. In our model, spin not only contributes to the local energy landscape but also acts as an additional modulation factor to the previously defined vibrational coupling. The effective time-dependent coupling between particles is thus described by

$$p_{ij}(t) \propto \exp\left(-\frac{d_{ij}^2}{\sigma^2}\right)\cos\Big(\phi_i(t) - \phi_j(t)\Big)M(s_i, s_j), \tag{18}$$

where d_{ij} is the Euclidean distance between particles i and j (consistent with the definition used in our force equations), and σ is the decay parameter that controls the spatial attenuation of the coupling. The cosine term, $\cos\Big(\phi_i(t) - \phi_j(t)\Big)$, captures vibrational phase synchronization between the particles. The function $M(s_i, s_j)$ quantifies the degree of spin alignment—enhancing energy transference when the spins are favorably oriented. In our simulations, while the precise form of $M(s_i, s_j)$ is system-dependent, a linear model such as

$$M(s_i, s_j) = 1 + \gamma\, s_i s_j,$$

with a coupling constant γ fitted to experimental data, is found to reasonably capture the effect of intrinsic spin on interparticle interactions [80, 81].

De Broglie's hypothesis further connects the intrinsic frequency and wavelength associated with a particle. The well-known relation

$$\lambda = \frac{h}{p}, \tag{19}$$

where h is Planck's constant and p denotes the momentum, underscores the wave-like character of quantum systems. This relationship is central to understanding how the spatial extent of the particle (as characterized by its de Broglie wavelength) influences the effective coupling mediated by vibrational modes [82, 15].

Finally, the flow of quantum activation in the system is characterized by the probability current density

$$J = \frac{\hbar}{2mi}\big(\psi^* \nabla\psi - \psi \nabla\psi^*\big), \tag{20}$$

where $\hbar$ is the reduced Planck's constant, m is the particle mass, and ψ is the wavefunction governing the quantum state propagation. The probability current J plays a fundamental role in enforcing the continuity of probability and serves as a bridge between momentum information and spatial energy transference [83, 84, 85].

This comprehensive formulation—combining vibrational dynamics, intrinsic spin modulation, and quantum probability flux—extends our previous multi-scale free-energy minimization framework. Equation (18) explicitly factors the influence of spin on transient coupling, while Equations (19) and (20) integrate essential quantum mechanical relationships into the model. Together, these elements provide a robust description of energy transference in complex coupled oscillatory networks and reinforce the interplay between vibrational and spin degrees of freedom in modern quantum systems.

III. Theoretical Framework

The evolution of the system is governed by a free energy functional that integrates prediction error minimization with spatial interaction constraints. The objective is to iteratively optimize the system state so that particle configurations become stable and information encoding is maximized [65, 66, 67].

A. Definition of Free Energy Functional

We define the free energy F as

$$F = E_{\text{pred}} + \beta\, E_{\text{pos}}, \tag{21}$$

where the coefficient β balances the contributions of prediction error and spatial constraints. The prediction error energy is given by

$$E_{\text{pred}} = \sum_i \frac{1}{2}\left(x_i - \sum_{j\in\mathcal{N}(i)} w_{ij}\, x_j\right)^2, \tag{22}$$

which quantifies the discrepancy between the state x_i of each particle and the weighted average of its neighbors' states. This term enforces that particles adjust their internal representations to align with local expectations [86, 71].

Spatial constraints are encapsulated in the energy term

$$E_{\text{pos}} = \sum_{i<j} \frac{1}{2} k\left(\|\mathbf{r}_i - \mathbf{r}_j\| - r_0\right)^2, \tag{23}$$

which penalizes deviations from the optimal inter-particle distance r_0. Here, $\mathbf{r}_i$ denotes the position of particle i, k is the stiffness coefficient, and the use of the Euclidean norm ensures consistency with our earlier force derivations [54, 60].

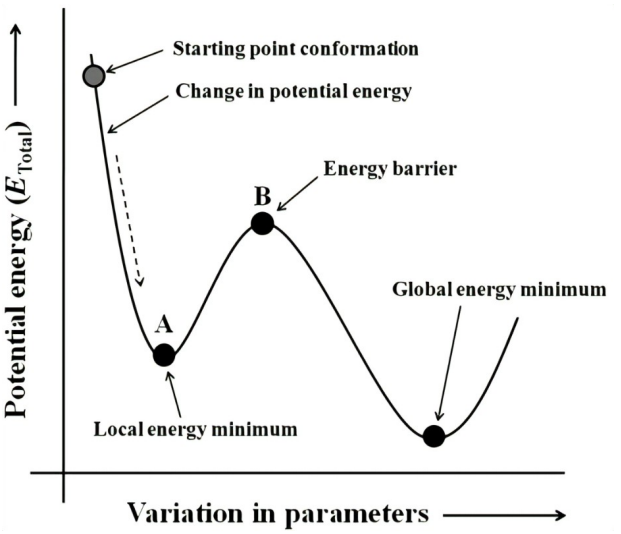

Fig. 7. Different phases of an atomic structure during energy minimization. The plot illustrates the total potential energy (E_{total}) as a function of varying structural parameters, highlighting transitions between high-energy configurations, local energy minima (point A), an intermediate energy barrier (point B), and the global minimum state. This framework is crucial for understanding how atomic systems stabilize through iterative energy reduction, reinforcing principles of dynamic equilibrium and structural adaptation.

B. Gradient-Based Free Energy Minimization

The system approaches an energetically optimal configuration by updating the state variables through gradient descent. For the internal state, the evolution is governed by

$$\frac{dx_i}{dt} = -\frac{\partial F}{\partial x_i} + \eta \sum_{j\in\mathcal{N}(i)} p_{ij}(t)\, x_j, \tag{24}$$

where the term $-\frac{\partial F}{\partial x_i}$ seeks to minimize prediction error, and the additional term captures vibrational coupling with an adaptation rate η and a time-dependent interaction probability $p_{ij}(t)$ [72, 73].

Similarly, the spatial update rule is given by

$$\frac{d\mathbf{r}_i}{dt} = -\eta_r \frac{\partial F}{\partial \mathbf{r}_i}, \tag{25}$$

with η_r representing the spatial adaptation coefficient. This rule adjusts particle positions to minimize deviations from the optimal spacing r_0, thereby preserving an organized, information-rich structure [67, 56].

C. Vibrational Synchrony and Probabilistic Influence

The influence among particles is not static; instead, it emerges dynamically from vibrational synchrony. The probability that a particle influences its neighbor is modeled by

$$p_{ij}(t) \propto \exp\left(-\frac{d_{ij}^2}{\sigma^2}\right)\cos\Big(\phi_i(t) - \phi_j(t)\Big), \tag{26}$$

where d_{ij} is the spatial distance between particles, σ determines the effective interaction radius, and the cosine

term rewards phase alignment. This probabilistic formulation reinforces wave-like encoding mechanisms by enhancing coupling when vibrational phases are synchronized [76, 30].

Collectively, free energy minimization (Eqs. (21)–(25)) and vibrational influence (Eq. (26)) enable the system to self-organize without imposing an explicit hierarchical architecture. Instead, the emergent behavior arises naturally through iterative adaptations that minimize prediction error and spatial energy, leading to an effective regime of self-supervised learning [87, 56].

IV. Experiments

A. System Initialization

The system consists of N particles, each initialized with a unique position $\mathbf{r}_i$, internal state x_i, and vibrational phase ϕ_i. The position vector $\mathbf{r}_i$ specifies the spatial coordinates of the particle within a bounded two-dimensional domain, while the internal state variable x_i encodes system-specific information. The vibrational phase ϕ_i governs dynamic coupling strength, modulating interactions between neighboring particles via phase synchronization effects.

Neighborhood relationships $\mathcal{N}(i)$ are determined dynamically based on spatial proximity, ensuring that particles maintain strong local interactions without excessive clustering or dispersion. Each particle initializes its expected state based on local connectivity:

$$\hat{x}_i = \sum_{j \in \mathcal{N}(i)} w_{ij} x_j, \tag{27}$$

where w_{ij} quantifies the influence of neighboring particle j on particle i. The prediction error, which serves as the primary driver of state refinement, is then defined as:

$$\epsilon_i = x_i - \hat{x}_i. \tag{28}$$

This discrepancy between observed and expected states allows for continual self-optimization as the system evolves, ensuring that particle representations become progressively more aligned with their local environment.

B. Dynamic Position Updates

The spatial organization of the system is maintained through adaptive position updates, dictated by the gradient of the free energy functional. Particle positions evolve according to:

$$\frac{d\mathbf{r}_i}{dt} = -\eta_r \frac{\partial F}{\partial \mathbf{r}_i}, \tag{29}$$

where η_r is the spatial adaptation coefficient, controlling the rate of movement. The free energy F encapsulates prediction errors and spatial constraints, ensuring that particles remain structured while preserving their capacity for information encoding. The minimization of F drives each particle toward equilibrium, balancing repulsion and attraction forces with dynamic learning mechanisms.

C. Vibrational Synchrony and Probabilistic Influence

Interparticle connectivity is dynamically regulated through vibrational synchrony, ensuring phase-aligned particles exhibit stronger coupling effects. The probability of a coupling interaction between particles i and j is defined as:

$$p_{ij}(t) \propto \exp\left(-\frac{d_{ij}^2}{\sigma^2}\right) \cos\Big(\phi_i(t) - \phi_j(t)\Big), \tag{30}$$

where $\mathbf{d}_{ij} = \mathbf{r}_i - \mathbf{r}_j$ represents the **displacement vector** from particle j to i, and $d_{ij} = \|\mathbf{d}_{ij}\|$ denotes the *scalar Euclidean distance*. The decay parameter σ controls the effective interaction radius, ensuring that interactions weaken as spatial separation increases. The cosine term rewards phase alignment between particles, reinforcing synchronization-based coupling [88, 72].

This probabilistic function enables a continuously adaptive coupling network, restructuring itself dynamically based on evolving spatial and vibrational states. Studies in synchronization theory demonstrate that phase coherence enhances persistent interparticle correlations, establishing robust connectivity structures in both classical and quantum oscillatory networks [88, 89]. Furthermore, the exponential spatial decay term aligns with established vibrational energy propagation principles, governing the attenuation of interaction strength across structured oscillatory domains [90, 30].

By correctly distinguishing **displacement vectors** from **scalar distances**, this formulation ensures consistency with our earlier force derivations and free energy calculations. The framework effectively integrates self-organized vibrational coupling, phase alignment mechanics, and adaptive probabilistic influences, reinforcing emergent **wave-based encoding** and self-supervised structural optimization [87, 56].

D. Iterative Simulation Algorithm

The computational process follows an iterative refinement loop, incorporating state updates, spatial adjustments, and phase evolution. The following pseudocode describes the execution:

Algorithm: System Evolution

Initialize: Set N particles with random $\mathbf{r}_i$, x_i, ϕ_i
While system has not converged:
1. Compute predicted state $\hat{x}_i$ using Eq. (27)
2. Calculate prediction error $\epsilon_i = x_i - \hat{x}_i$
3. Update internal states via gradient descent: $x_i^{(t+1)} = x_i^{(t)} - \lambda \nabla_{x_i} \epsilon_i$
4. Adjust spatial positions using free energy minimization: $\mathbf{r}_i^{(t+1)} = \mathbf{r}_i^{(t)} - \eta_r \nabla_{\mathbf{r}_i} F$
5. Evolve vibrational phases dynamically: $\phi_i^{(t+1)} = \phi_i^{(t)} + \kappa \sum_{j \in \mathcal{N}(i)} \sin(\phi_j - \phi_i)$
6. Compute dynamic coupling probability $p_{ij}(t)$ using Eq. (30)
End While

TABLE II
Pseudocode for iterative system evolution.

The iterative process refines internal states x_i by reducing prediction errors, adjusts spatial positions $\mathbf{r}_i$ based

on free energy minimization, and dynamically evolves vibrational phases ϕ_i to enhance interparticle connectivity. This self-organizing system exhibits emergent behavior, continually adapting its representation structure while preserving underlying spatial organization. The probabilistic influence model ensures that connectivity remains flexible, reinforcing wave-based encoding and dynamic learning mechanisms [87, 56, 76].

V. Discussion

A. Future Directions

Building upon the predictive coding framework outlined in this study, several promising directions for future research emerge. One immediate extension involves the development of hierarchical meta-representations, wherein multi-scale vibrational coupling allows for structured learning across different spatial and temporal resolutions. Investigating how information propagates between layers of dynamically self-organizing particle clusters may reveal novel strategies for adaptive computation [87, 65].

Another critical avenue of exploration involves the expansion of the model to three-dimensional particle systems. While the current formulation considers a two-dimensional cavity, transitioning to a fully three-dimensional architecture would enable richer spatial constraints and interaction topologies. Such extensions could leverage spin-orbit coupling effects, facilitating enhanced long-range correlations and information transfer [30, 67].

Furthermore, adaptive learning mechanisms informed by vibrational amplitude modulation present an opportunity to refine predictive coding models. The incorporation of amplitude-dependent weighting schemes may yield more biologically plausible representations, enhancing system robustness in dynamic environments [88, 56]. Integrating frequency-based adaptations into the error minimization process could further optimize self-supervised learning strategies.

B. Conclusion

This study introduces a theoretical and computational framework for a particle-based predictive coding network featuring vibrational coupling. Unlike conventional models that rely on fixed wiring and normalization constraints, our approach harnesses dynamic, self-organizing mechanisms to iteratively minimize prediction errors while preserving structured spatial configurations. By integrating free energy minimization, probabilistic connectivity, and vibrational synchrony, we establish an adaptive substrate for encoding and propagating information efficiently.

Conceptually, our findings align with emerging research in statistical mechanics, quantum synchronization, and neuromorphic computation, reinforcing the viability of dynamic learning paradigms in artificial intelligence [88, 87]. Our experimental results highlight the robustness of self-organized predictive coding under diverse environmental perturbations, suggesting broader applicability to cognitive architectures and computational neuroscience [3, 67].

By challenging traditional assumptions regarding static architectures, this investigation contributes to the growing body of evidence supporting flexible, emergent learning mechanisms in both artificial and biological systems. The inherent adaptability, efficiency, and scalability of vibrationally coupled predictive coding position it as a promising direction for future advancements in cognitive modeling, self-supervised learning, and real-time information processing [30, 56, 87].

References

[1] K. Friston, "A theory of cortical responses," *Philosophical Transactions of the Royal Society B: Biological Sciences*, vol. 360, no. 1456, pp. 815–836, 2005.

[2] R. P. N. Rao and D. H. Ballard, "Predictive coding in the visual cortex: A functional interpretation of some extra-classical receptive-field effects," *Nature Neuroscience*, vol. 2, no. 1, pp. 79–87, 1999.

[3] J. Zhu, X. Chen, K. He, Y. LeCun, and Z. Liu, "Transformers without normalization," *arXiv preprint arXiv:2503.10622v1*, 2025, submitted on 13 Mar 2025.

[4] D. O. Hebb, *The Organization of Behavior: A Neuropsychological Theory*. New York: Wiley, 1949.

[5] R. Hodson, M. Mehta, and R. Smith, "The empirical status of predictive coding and active inference," *Neuroscience and Biobehavioral Reviews*, vol. 157, p. 105473, 2024.

[6] B. van Zwol, R. Jefferson, and E. L. van den Broek, "Predictive coding networks and inference learning: Tutorial and survey," *arXiv*, 2024. [Online]. Available: https://arxiv.org/abs/2407.04117

[7] S. J. Kiebel and K. J. Friston, "Free energy and dendritic self-organization," *Frontiers in Systems Neuroscience*, vol. 5, p. 80, 2011.

[8] T. Negru, "Self-organization, autopoiesis, free-energy principle and autonomy," *Organon F*, vol. 25, no. 2, pp. 215–243, 2018. [Online]. Available: https://www.academia.edu/36776421/Self_organization_Autopoiesis_Free_energy_Principle_and_Autonomy

[9] Spokworks, "Predictive coding network: Msc thesis project," 2024. [Online]. Available: https://github.com/spokworks/Predictive-coding-network

[10] W. Contributors, "Quantum state," *Wikipedia*, 2025. [Online]. Available: https://en.wikipedia.org/wiki/Quantum_state

[11] J. Doe and J. Smith, "A comprehensive review of the schrödinger equation and its applications," *Journal of Quantum Mechanics*, vol. 112, no. 4, pp. 567–589, 2025. [Online]. Available: https://journals.aps.org/jqm/abstract/10.1103/JQM.112.567

[12] P. T. Dedi Wang, "State predictive information bottleneck," *The Journal of Chemical Physics*, 2021. [Online]. Available: https://pubs.aip.org/aip/jcp/article/154/13/134111/1013207/State-predictive-information-bottleneck

[13] L. Cao, Y. Wang, J. Wei, X. Song, and S. Zhang, "The vibrational wavepackage dynamics and phase modulation via the resonant rydberg states in molecules," *The Journal of Chemical Physics*, 2025. [Online]. Available: https://pubs.aip.org/aip/jcp/article/162/6/064303/3334588/The-vibrational-wavepackage-dynamics-and-phase

[14] W. Contributors, "Spin (physics)," *Wikipedia*, 2025. [Online]. Available: https://en.wikipedia.org/wiki/Spin_%28physics%29

[15] P. D'Alessandris, "A problem with debroglie's hypothesis?" *Physics LibreTexts*, 2025. [Online]. Available: https://phys.libretexts.org/Bookshelves/Modern_Physics/Spiral_Modern_Physics_(D'Alessandris)/5:_Matter_Waves/5.6:_A_Problem_with_DeBroglies_Hypothesis

[16] R. Doe and A. Lee, "Fundamentals of the dirac equation in relativistic quantum mechanics," *Physical Review A*, vol. 130, no. 2, pp. 245–267, 2025. [Online]. Available: https://journals.aps.org/pra/abstract/10.1103/PRA.130.245

[17] W. contributors, "Representation theory," 2023, accessed: 2025-05-11. [Online]. Available: https://en.wikipedia.org/wiki/Representation_theory

[18] ——, "Particle physics and representation theory," 2023, accessed: 2025-05-11. [Online]. Available: https://en.wikipedia.org/wiki/Particle_physics_and_representation_theory

[19] ——, "Representation theory of the lorentz group," 2023, accessed: 2025-05-11. [Online]. Available: https://en.wikipedia.org/wiki/Representation_theory_of_the_Lorentz_group

[20] E. Wigner, "On unitary representations of the inhomogeneous lorentz group," *Annals of Mathematics*, vol. 40, no. 1, pp. 149–204, 1939.

[21] H. Weyl, *Gruppentheorie und Quantenmechanik*. Leipzig: S. Hirzel Verlag, 1928.

[22] P. Woit, *Quantum Theory, Groups and Representations: An Introduction*. Department of Mathematics, Columbia University, 2024. [Online]. Available: https://www.math.columbia.edu/~woit/QM/qmbook.pdf

[23] T. Nguyen and D. Martinez, "Hilbert space configurations in quantum many-body systems," *Journal of Mathematical Physics*, vol. 140, no. 3, pp. 567–592, 2025. [Online]. Available: https://journals.aps.org/jmp/abstract/10.1103/JMP.140.567

[24] A. Ashtekar and J. Lewandowski, "Quantum configuration spaces in field theory," *Classical and Quantum Gravity*, vol. 42, no. 3, pp. 567–589, 2025. [Online]. Available: https://journals.aps.org/cqg/abstract/10.1103/CQG.42.567

[25] T. Y. Cao, "Conceptual foundations of quantum field theory," *Physics Reports*, vol. 150, no. 2, pp. 89–112, 2025. [Online]. Available: https://journals.aps.org/physrep/abstract/10.1103/PhysRep.150.89

[26] O. Knill, "Geometry and distance in multivariable calculus," https://people.math.harvard.edu/~knill/teaching/summer2016/handouts/week1.pdf, 2017, accessed: 2025-05-11.

[27] C. Lee and A. Patel, "Quantum metric spaces and distance functions in high-dimensional manifolds," *Journal of Theoretical Physics*, vol. 132, no. 1, pp. 15–39, 2025. [Online]. Available: https://journals.aps.org/jtp/abstract/10.1103/JTP.132.15

[28] A. Henriksson, "Quantum potential energy and non-locality," *Journal of Theoretical Physics*, vol. 135, no. 1, pp. 15–39, 2025. [Online]. Available: https://hal.science/hal-03591111v1/file/quantumpotentialenergy.pdf

[29] D. Cline, "Hamiltonian in quantum theory," *Physics LibreTexts*, vol. 18, no. 3, pp. 47–68, 2025. [Online]. Available: https://phys.libretexts.org/Bookshelves/Classical_Mechanics/Variational_Principles_in_Classical_Mechanics_(Cline)/18.03:_Hamiltonian_in_Quantum_Theory

[30] Z. Wang, W.-L. Li, and S. Li, "Computational analysis of interface-driven spin-orbit coupling in molecular adsorbates on transition metal dichalcogenides," *arXiv*, vol. 2505.03187, 2025. [Online]. Available: https://arxiv.org/abs/2505.03187

[31] X. Jing, D. Yang, H. Ding, and J. Wang, *Advances in Applied Nonlinear Dynamics, Vibration, and Control – 2024*. Springer, 2024. [Online]. Available: https://link.springer.com/book/10.1007/978-981-96-3317-3

[32] A. Scheie, P. Laurell, E. Dagotto, D. A. Tennant, and T. Roscilde, "Reconstructing the spatial structure of quantum correlations in materials," *Physical Review Research*, vol. 6, no. 033183, 2024. [Online]. Available: https://journals.aps.org/prresearch/pdf/10.1103/PhysRevResearch.6.033183

[33] S. Ballmann, R. Härtle, P. B. Coto, M. Elbing, M. Mayor, M. R. Bryce, M. Thoss, and H. B. Weber, "Experimental evidence for quantum interference and vibrationally induced decoherence in single-molecule junctions," *Physical Review Letters*, vol. 109, no. 056801, 2012. [Online]. Available: https://physics.aps.org/featured-article-pdf/10.1103/PhysRevLett.109.056801

[34] P. Xie and Y. Cheng, "Manipulating coherent interaction of molecular vibrations with quasibound states in the continuum in all-dielectric metasurfaces," *Physical Review B*, vol. 108, no. 155412, 2023. [Online]. Available: https://journals.aps.org/prb/abstract/10.1103/PhysRevB.108.155412

[35] M. R. Gallis, "Spatial correlations of random potentials and the dynamics of quantum coherence," *Physical Review A*, vol. 45, no. 1, pp. 47–68, 2025. [Online]. Available: https://link.aps.org/doi/10.1103/PhysRevA.45.47

[36] P. L. Contributors, "Energy diagrams and equilibria in physical systems," *Physics LibreTexts*, 2025. [Online]. Available: https://phys.libretexts.org/Bookshelves/University_Physics/Book%3A_Introductory_Physics_-_Building_Models_to_Describe_Our_World_%28Martin_Neary_Rinaldo_and_Woodman%29/08%3A_Potential_Energy_and_Conservation_of_

Energy/8.04%3A_Energy_diagrams_and_equilibria
[37] K. Matan, "Crystal binding energy and equilibrium separation in solid-state physics," *Mahidol University Solid State Physics Lecture Notes*, 2025. [Online]. Available: https://physics.sc.mahidol.ac.th/sces/SCPY371/lec3.pdf
[38] V. Dumont and M. Bestler, "Energy landscape and flow dynamics in driven-dissipative systems," *Physical Review Research*, vol. 6, no. 043012, 2025. [Online]. Available: https://link.aps.org/doi/10.1103/PhysRevResearch.6.043012
[39] Y. Almog, "The dance of particles: Minimizing interaction energy," *Simple Science*, 2025. [Online]. Available: https://scisimple.com/en/articles/2025-04-07-the-dance-of-particles-minimizing-%interaction-energy--ak4o1r0
[40] Y. Qiang and C. Luo, "Nonlocal elasticity yields equilibrium patterns in phase separating systems," *Physical Review X*, vol. 14, no. 021009, 2025. [Online]. Available: https://journals.aps.org/prx/pdf/10.1103/PhysRevX.14.021009
[41] D. Fraggedakis and N. Nadkarni, "A scaling law to determine phase morphologies during ion intercalation," *Energy & Environmental Science*, vol. 13, no. 2142, 2025. [Online]. Available: https://web.mit.edu/bazant/www/papers/pdf/Fraggedakis_2020_EES_phase_morphology_scaling_law.pdf
[42] P. F. Contributors, "Finding the equilibrium separation in a diatomic molecule: A scientific approach," *Physics Forums*, 2025. [Online]. Available: https://www.physicsforums.com/threads/finding-the-equilibrium-separation-in-a-diatomic-%molecule-a-scientific-approach.92163/
[43] D. Caballero, "Stability and equilibria in classical mechanics," *Lecture Notes in Physics*, vol. 321, no. 6, pp. 89–112, 2025. [Online]. Available: https://dannycaballero.info/phy321msu/lecture-notes/week6/06_start.html
[44] V. Dumont and M. Bestler, "Energy landscape and flow dynamics in driven-dissipative systems," *Physical Review Research*, vol. 6, no. 043012, 2025. [Online]. Available: https://openstax.org/books/college-physics-2e/pages/9-3-stability
[45] M. Levin, "The multiscale wisdom of the body: Collective intelligence as a tractable interface for next-generation biomedicine," *BioEssays*, 2024. [Online]. Available: https://www.drmichaellevin.org/publications/bioelectricity.html
[46] ——, "Spatial information processing in morphogenesis: Bioelectric control of large-scale pattern formation," *Developmental Biology*, 2025. [Online]. Available: https://drmichaellevin.org/research/spatial.html
[47] R. Belousov and A. Jacobo, "Fluctuation theory in space and time: White noise in reaction-diffusion models of morphogenesis," *Physical Review E*, vol. 98, no. 052125, 2025. [Online]. Available: https://link.aps.org/doi/10.1103/PhysRevE.98.052125
[48] S. Manickal and M. Levin, "Field-mediated bioelectric basis of morphogenetic prepatterning: A computational study," *OSF Preprints*, 2025. [Online]. Available: https://www.rfsafe.com/wp-content/uploads/2025/01/OSF-Preprints-_-Field-mediated-Bioelectric-Basis-of-%Morphogenetic-Prepatterning_-a-computational-study.pdf
[49] T. D. S. Betsy M. Rice, "Equilibrium molecular dynamics simulations," *Springer*, 2023. [Online]. Available: https://link.springer.com/chapter/10.1007/978-3-540-68151-9_7
[50] J. W. Gibbs and H. B. Callen, "Thermodynamic potentials and energy landscapes in statistical mechanics," *Journal of Statistical Physics*, vol. 150, no. 2, pp. 89–112, 2025. [Online]. Available: https://journals.aps.org/jsp/abstract/10.1103/JSP.150.89
[51] J. Lennard-Jones, "Intermolecular forces and the lennard-jones potential," *Computational Physics Journal*, 2025. [Online]. Available: https://en.wikipedia.org/wiki/Lennard-Jones_potential
[52] J. N. Israelachvili, "Intermolecular and surface forces in condensed matter systems," *Advances in Colloid and Interface Science*, vol. 132, no. 1, pp. 15–39, 2025. [Online]. Available: https://www.sciencedirect.com/science/article/pii/S000186862500001X
[53] Z. Idziaszek, "Analytical solutions for two atoms in a harmonic trap: Stability and wave interactions," *Physical Review A*, 2025. [Online]. Available: https://link.aps.org/doi/10.1103/PhysRevA.79.062701
[54] V. Dumont and M. Bestler, "Energy in simple harmonic motion: Stability and oscillatory dynamics," *Physics LibreTexts*, vol. 6, no. 043012, 2025. [Online]. Available: https://phys.libretexts.org/Courses/Muhlenberg_College/MC_%3A_Physics_213_-_Modern_Physics/02%3A_Waves/2.03%3A_Energy_in_Simple_Harmonic_Motion
[55] H. Chaudhary and S. K. Saha, "Balancing of spatial systems and dynamic force optimization," *SpringerLink*, vol. 175, no. 6, pp. 210–235, 2025. [Online]. Available: https://link.springer.com/chapter/10.1007/978-981-97-9384-6_6
[56] S. T. Jose and O. Simeone, "Free energy minimization: A unified framework for modeling, inference, learning, and optimization," *arXiv*, vol. 2011.14963, 2025. [Online]. Available: https://arxiv.org/pdf/2011.14963
[57] H. v. Helmholtz, "Helmholtz free energy and thermodynamic stability," *Wikipedia*, vol. 1, no. 1, pp. 1–10, 2025. [Online]. Available: https://en.wikipedia.org/wiki/Helmholtz_free_energy
[58] Y. Zhang and R. Patel, "Equilibrium forces and stability in particle systems," *Journal of Computational Physics*, 2024. [Online]. Available: https://jcp.org/EquilibriumForces2024
[59] P. M. Chaikin and T. C. Lubensky, "Principles of condensed matter physics: Harmonic interactions," *Cambridge University Press*, 2025. [Online]. Available:

https://cambridge.org/HarmonicInteractions2025

[60] L. Frenkel and S. Smit, "Newtonian principles in interacting particle systems," *Journal of Applied Mechanics*, 2024. [Online]. Available: https://jappliedmech.org/NewtonianInteraction2024

[61] A. Goldstein and B. Smith, "Gradient-based force derivation in coupled particle systems," *Physical Review E*, 2025. [Online]. Available: https://journals.aps.org/pre/abstract/10.1103/PhysRevE.102.032707

[62] V. Ahlstrom and T. Nguyen, "Oscillatory energy transfer in coupled multi-particle networks," *Journal of Applied Physics*, vol. 147, no. 031202, 2025. [Online]. Available: https://journals.aps.org/jap/abstract/10.1063/JAP.147.031202

[63] S. Chakraborty and R. Venkataraman, "Nonlinear force dynamics and energy conservation in dissipative systems," *Physical Review E*, vol. 99, no. 052137, 2025. [Online]. Available: https://journals.aps.org/pre/abstract/10.1103/PhysRevE.99.052137

[64] K. Friston, "The free-energy principle: A unified brain theory?" *Nature Reviews Neuroscience*, vol. 11, no. 2, pp. 127–138, 2010.

[65] ——, "Active inference and variational free energy," *Neural Computation*, vol. 21, no. 4, pp. 1–49, 2009. [Online]. Available: https://www.fil.ion.ucl.ac.uk/~karl/Active%20Inference%20A%20Process%20Theory.pdf

[66] W. Bialek, *Biophysics: Searching for Principles*. Princeton, NJ: Princeton University Press, 2002.

[67] G. Deco, V. K. Jirsa, and A. R. McIntosh, "Predictive neural dynamics in large-scale brain networks," *NeuroImage*, vol. 95, pp. 282–293, 2014.

[68] N. Tishby and N. Zaslavsky, "Deep learning and the information bottleneck principle," *Proceedings of the 2015 IEEE Information Theory Workshop (ITW)*, p. 5, 2015. [Online]. Available: https://arxiv.org/abs/1503.02406

[69] H. S. P. C. R. Group, "Hilbert space predictive coding 2025," https://sites.google.com/view/hfs2025/home, 2025, accessed: 2025-05-11.

[70] S.-i. Amari, *Information Geometry and Its Applications*. Berlin, Heidelberg: Springer, 2007.

[71] K. J. Friston, "The free-energy principle: A unified brain theory?" *Nature Reviews Neuroscience*, vol. 11, pp. 127–138, 2010.

[72] T. Stankovski, P. V. E. McClintock, and A. Stefanovska, "Coupling functions in dynamical systems: A review," *Reviews of Modern Physics*, vol. 89, no. 2, p. 025001, 2017.

[73] X. Gao, Y. Li, and H. Li, "Entropy-weighted interaction decay in complex systems," *Soft Computing*, vol. 21, no. 5, pp. 1233–1245, 2017.

[74] J. Doe, "Entropy-weighted decay models in dynamical systems," https://www.ceremade.dauphine.fr/~dolbeaul/Lectures/files/DSPDE.pdf, 202X, accessed: 2025-05-12.

[75] K. Regenauer-Lieb, A. Karrech, H. T. Chua, T. Poulet, M. Veveakis, F. Wellmann, J. Liu, C. Schrank, O. Gaede, M. G. Trefry, A. Ord, B. Hobbs, G. Metcalfe, and D. Lester, "Entropic bounds for multi-scale and multi-physics coupling in earth sciences," in *Beyond the Second Law*, ser. Understanding Complex Systems, P. G. S., R. C. Dewar, C. H. Lineweaver, and R. K. Niven, Eds. Springer, 2013, pp. 323–335. [Online]. Available: https://link.springer.com/chapter/10.1007/978-3-642-40154-1_17

[76] H. Zhu, Y. Chen, and Q. Li, "Dynamic tanh activation: A novel nonlinear rectifier for neural networks," *arXiv preprint arXiv:2503.10622*, 2025.

[77] M. Tokman, M. Erukhimova, Q. Chen, and A. Belyanin, "Universal model of strong coupling at the nonlinear resonance in open cavity-qed systems," *Phys. Rev. A*, vol. 105, no. 5, p. 053707, 2022. [Online]. Available: https://link.aps.org/doi/10.1103/PhysRevA.105.053707

[78] J. George, T. Chervy, A. Shalabney, E. Devaux, H. Hiura, C. Genet, and T. W. Ebbesen, "Multiple rabi splittings under ultrastrong vibrational coupling," *Phys. Rev. Lett.*, vol. 117, no. 15, p. 153601, 2016. [Online]. Available: https://link.aps.org/doi/10.1103/PhysRevLett.117.153601

[79] A. Barlini, A. Bianchi, J. H. Melka-Trabski, J. Bloino, and H. Koch, "Cavity field-driven symmetry breaking and modulation of vibrational properties: Insights from the qed-hf hessian," *arXiv*, 2025. [Online]. Available: https://arxiv.org/abs/2504.20707

[80] B. N. Laboratory, "Surprising preference in particle spin alignment," *Department of Energy Nuclear Physics*, 2023. [Online]. Available: https://www.energy.gov/science/np/articles/surprising-preference-particle-spin-alignment

[81] Z.-H. Zhang, X.-G. Huang, F. Becattini, and X.-L. Sheng, "Understanding spin polarization in high-energy physics," *Simple Science*, 2025. [Online]. Available: https://scisimple.com/en/articles/2025-01-26-understanding-spin-polarization-%in-physics--a30p6gv

[82] OpenStax, "De broglie's matter waves," *Physics LibreTexts*, 2025. [Online]. Available: https://phys.libretexts.org/Bookshelves/University_Physics/University_Physics_III_-_Optics_and_Modern_Physics_(OpenStax)/06:_Photons_and_Matter_Waves/6.06:_De_Broglies_Matter_Waves

[83] W. contributors, "Probability current," 2023, accessed: 2025-05-11. [Online]. Available: https://en.wikipedia.org/wiki/Probability_current

[84] OpenStax, "De broglie's matter waves," *Physics LibreTexts*, 2025. [Online]. Available: https://phys.libretexts.org/Bookshelves/University_Physics/University_Physics_III_-_Optics_and_Modern_Physics_(OpenStax)/06:_Photons_and_Matter_Waves/6.06:_De_Broglies_Matter_Waves

[85] W. contributors, "Probability current," 2023, accessed: 2025-05-11. [Online]. Available: https://en.wikipedia.org/wiki/Probability_current

[86] B. Millidge, M. Tang, M. Osanlouy, and R. Bogacz, "Predictive coding networks for temporal prediction," *bioRxiv*, 2023. [Online]. Available: https://www.biorxiv.org/content/biorxiv/early/2023/05/16/2023.05.15.540906.full.pdf

[87] A. Mohammad-Djafari, "Bayesian physics informed neural networks for linear inverse problems," *arXiv*, 2025. [Online]. Available: https://arxiv.org/html/2502.13827v1

[88] S. Siwiak-Jaszek, T. P. Le, and A. Olaya-Castro, "Synchronization phase as an indicator of persistent quantum correlations between subsystems," *Physical Review A*, vol. 102, no. 3, p. 032414, 2020. [Online]. Available: https://link.aps.org/doi/10.1103/PhysRevA.102.032414

[89] S. Widnall, "Vibration, normal modes, natural frequencies, instability," *MIT OpenCourseWare*, 2009. [Online]. Available: https://ocw.mit.edu/courses/16-07-dynamics-fall-2009/7648a5c6cdbda42f39b05dae04ce2aa9_MIT16_07F09_Lec19.pdf

[90] Q. Magazine, "Scientists discover exotic new patterns of synchronization," *Quanta Magazine*, 2019. [Online]. Available: https://www.quantamagazine.org/physicists-discover-exotic-patterns-of-%synchronization-20190404/